

## The CALorimetric Electron Telescope (CALET)<sup>(1)</sup>

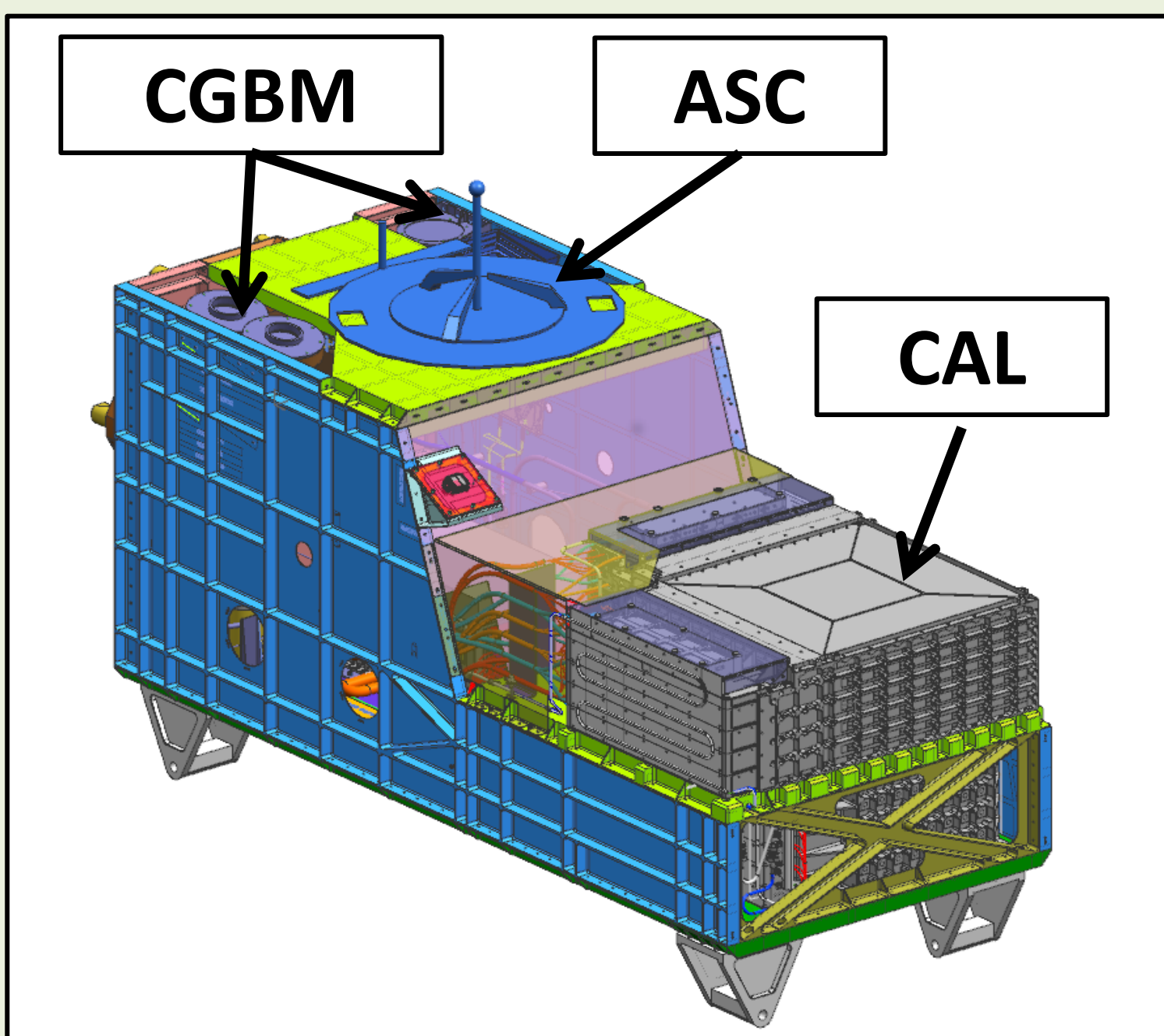


Figure 1: CALET structure indicating the CALET Gamma-ray Burst Monitor (CGBM), Advanced Stellar Compass (ASC), and CALET Calorimeter (CAL).

Component	Description	Function
CHD	<ul style="list-style-type: none"> <li>Plastic scintillating paddles</li> <li>14 paddles x 2 layers (X, Y) = 28 paddles</li> <li>Each paddle: 32 x 10 x 450 mm<sup>3</sup></li> </ul>	Charge Measurement
IMC	<ul style="list-style-type: none"> <li>Plastic scintillating fibers &amp; tungsten plates</li> <li>448 fibers x 16 layers (8X, 8Y) = 7168 fibers</li> <li>Each fiber: 1 x 1 x 448 mm<sup>3</sup></li> <li>7 W layers: (5 x 0.2 X<sub>0</sub>) + (2 x 1 X<sub>0</sub>) = 3 X<sub>0</sub></li> </ul>	Particle Tracking
TASC	<ul style="list-style-type: none"> <li>Lead tungstate (PbWO<sub>4</sub>; PWO) logs</li> <li>16 logs x 12 layers (6X, 6Y) = 192 logs</li> <li>Each log: 19 x 20 x 326 mm<sup>3</sup></li> <li>Total thickness: 27 X<sub>0</sub>, ~1.2 λ<sub>i</sub></li> </ul>	Energy reconstruction

## CALET Ultra-Heavy Analysis Dataset

- CALET uses dedicated UH trigger<sup>(2)</sup> which only requires events pass through CHD and top of IMC
- FOV increased from ~45 to ~75 degrees, increasing geometric factor to ~4000 cm<sup>2</sup> sr
- 1.8 x 10<sup>8</sup> UH events collected between October 2015 and September 2020

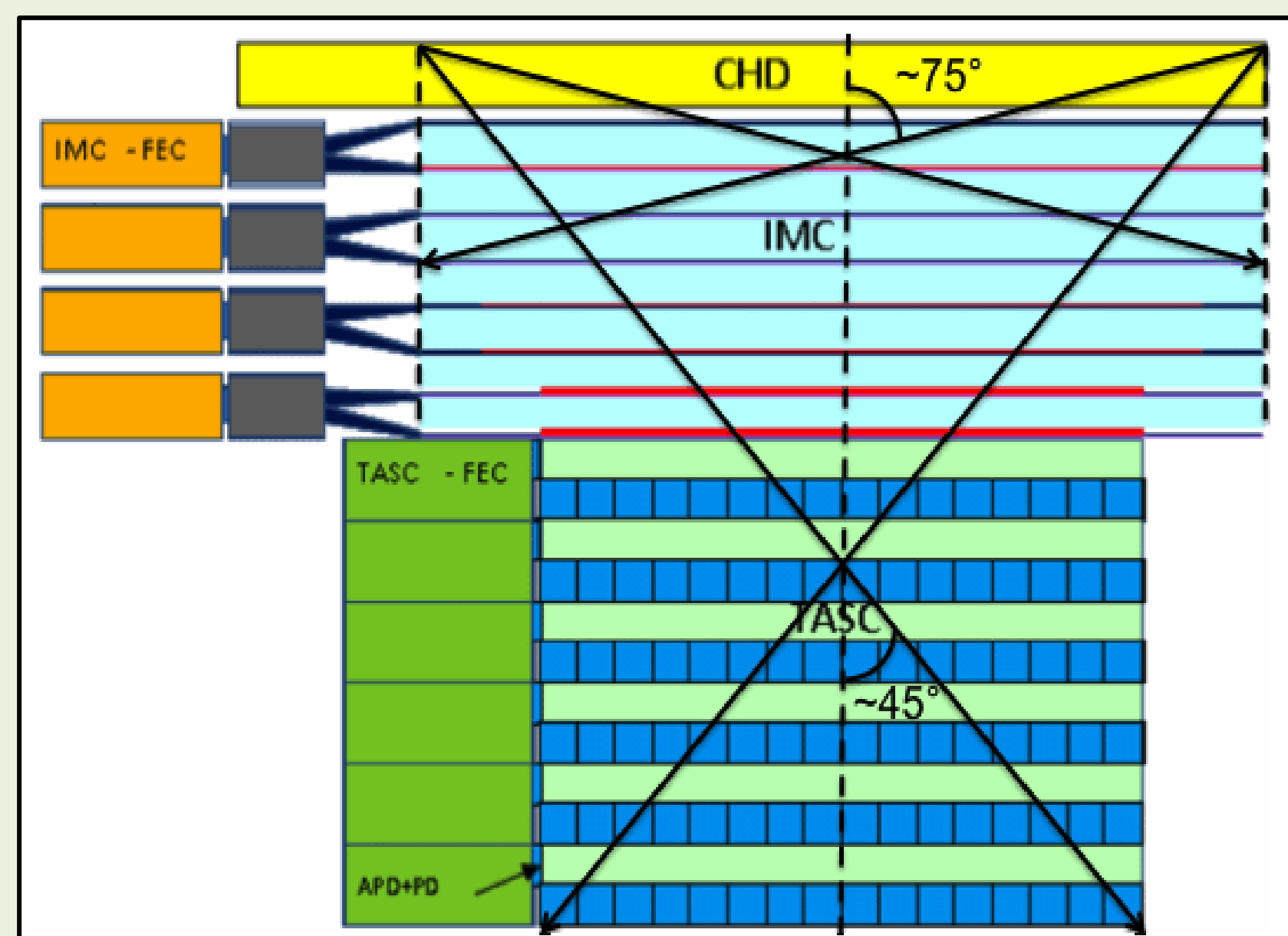


Figure 2: Diagram of the CAL showing the approximate geometry requirements of the standard and UH trigger modes.

## Event Selection

- Theta Cut<sup>(3)</sup>: Events must have a reconstructed UH track with incidence angle of less than 60 degrees
- Charge Consistency<sup>(3)</sup>: Difference in estimated charges in the CHDX and CHDY for each event can not exceed 1.5%

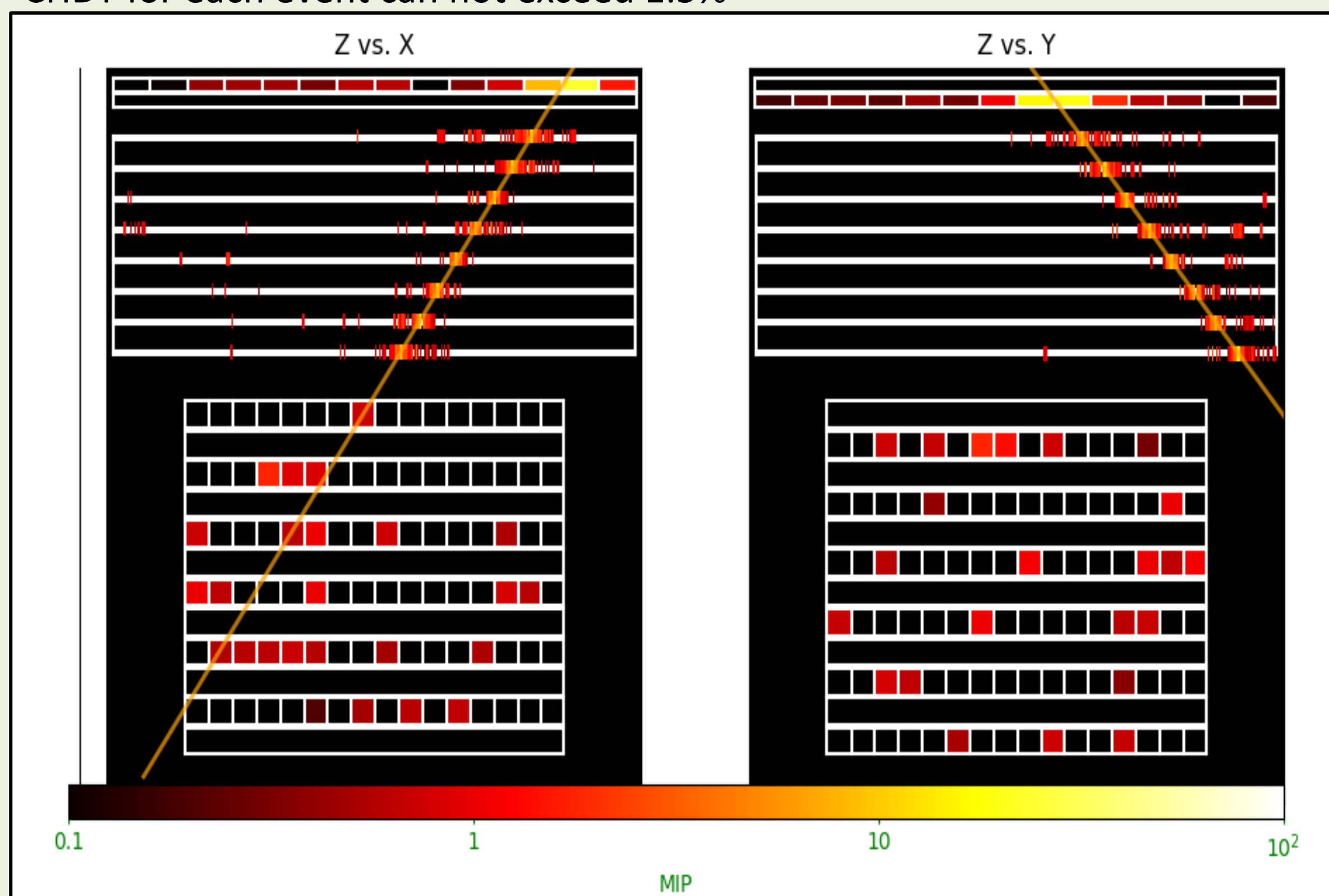


Figure 3: Ultra-heavy nuclei event candidate visualized with the CALET event viewer.

## Charge Correction of Ultra-heavy Events

### Time Dependence

- Cause:**
- Changes in temperature
  - Long-term gain drift
- Correction:**
- Perform Si and Fe peak fits in 1-day bins
  - Apply linear correction

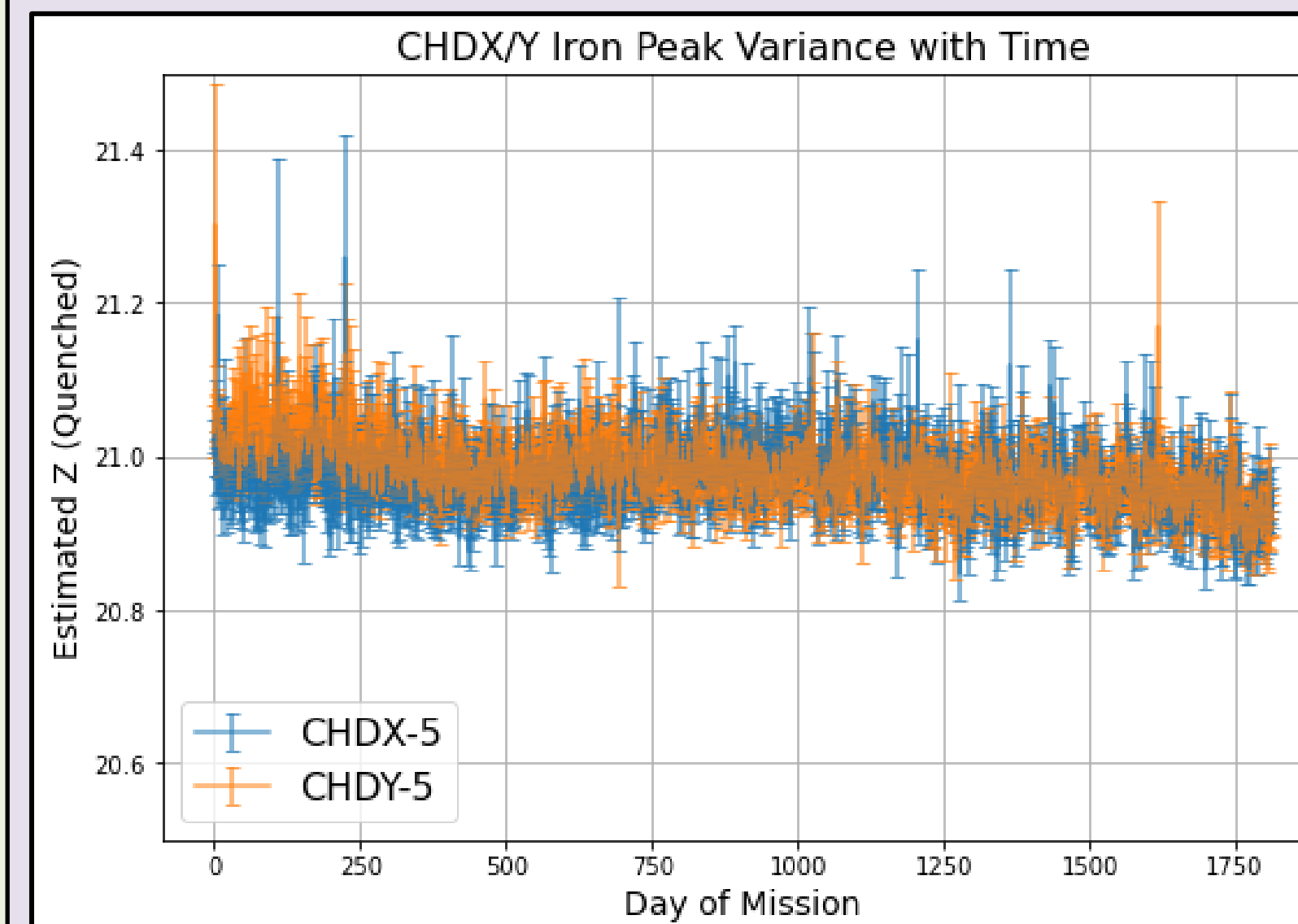


Figure 4: Location of the fitted Fe peak for CHDX and CHDY for each day in the UH dataset.

### Spatial Dependence

- Cause:**
- Light propagation effects
  - Material non-uniformity
- Correction:**
- Perform Si and Fe peak fits in 3.2 x 3.2 cm bins in the CHDX and CHDY.
  - Apply linear correction

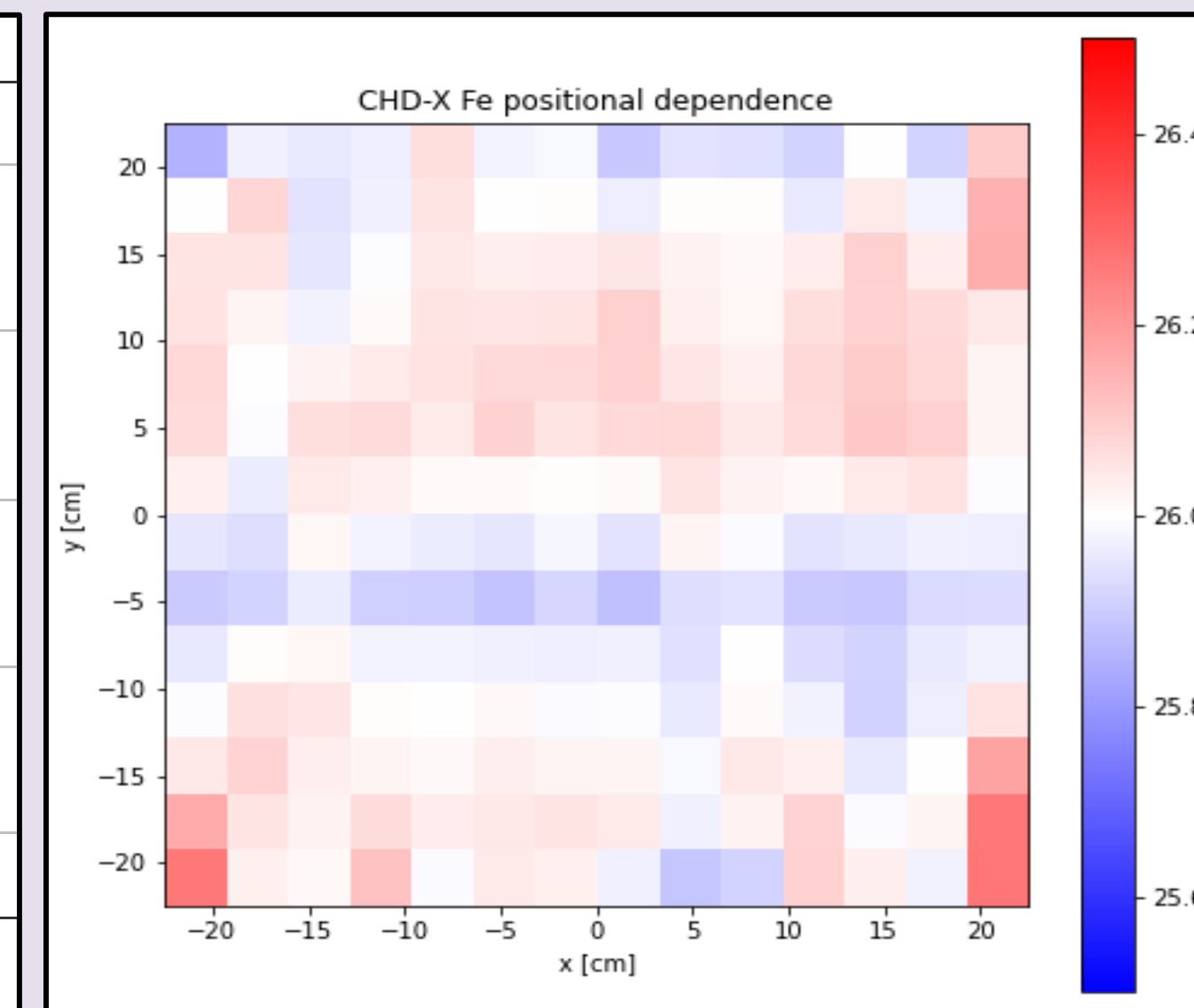


Figure 5: Location of the fitted Fe peak for each position bin of the CHDX.

## Quenching Correction

### Time and Position Corrected UH Spectrum

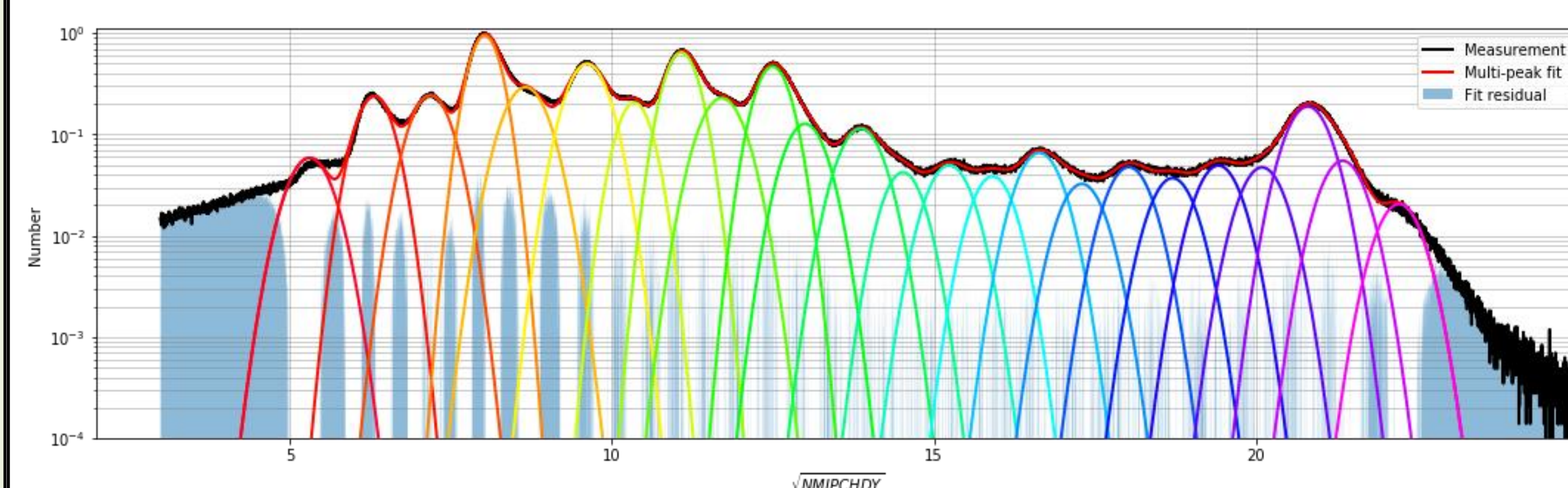


Figure 6: Resulting quenched UH spectrum following time and position corrections.

- Multi-peak fit from C to Ni
- Fit Tarle function to peaks to find parameters.
- Invert Tarle function to return corrected dE/dx values

$$\frac{dE}{dx} = \frac{B_1 Z^2}{1 + B_2 Z^2} + B_3 Z^2$$

### Position/Time Corrected Dequenched UH Spectra

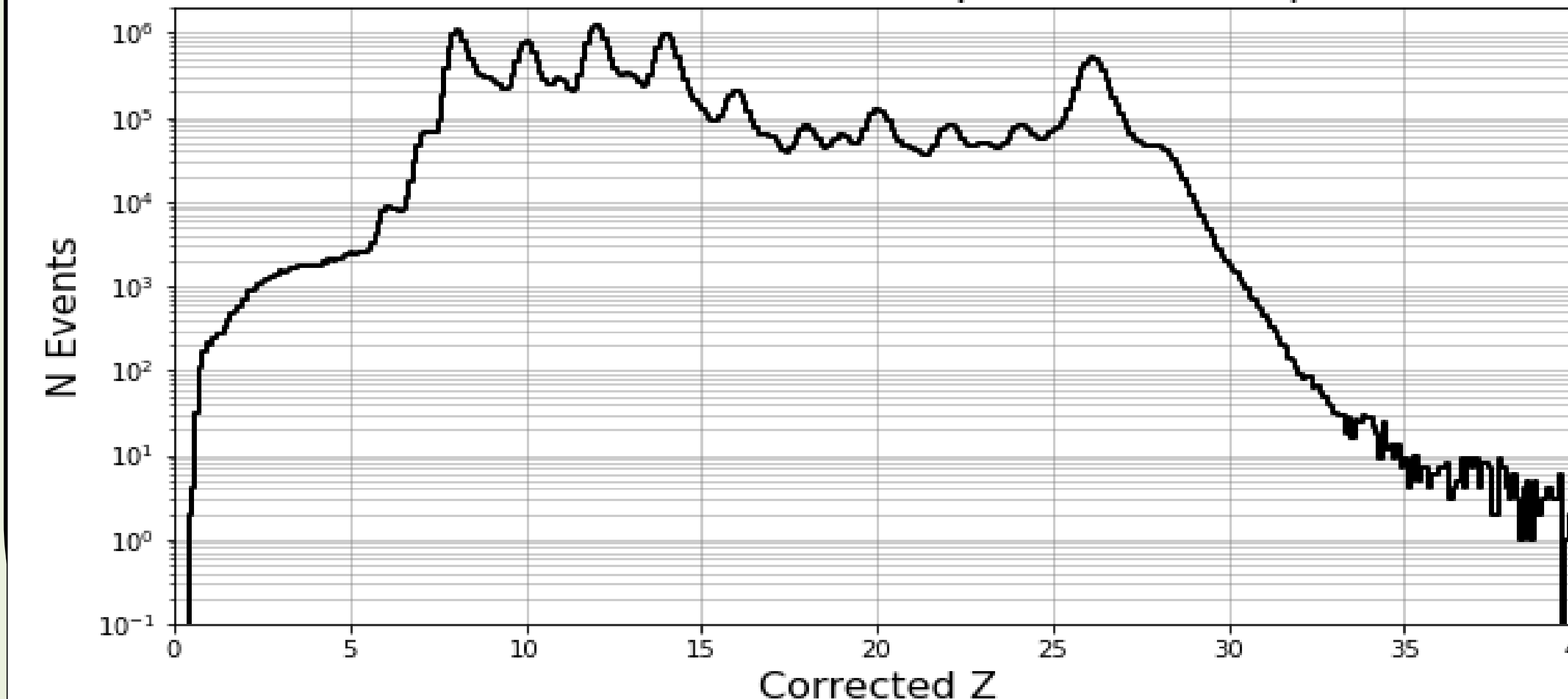


Figure 7: Resulting charge corrected UH spectrum following time and position corrections.

## Removing Non-relativistic and Low Z Nuclei Contamination

### Challenge

- Non-relativistic nuclei lead to higher ionization energy deposits
  - Along with low Z nuclei, this causes contamination in the UH dataset
- Methods**
- Remove observations made at times of low cutoff rigidity
  - Make direct cut on energy deposits in the TASC (see reference 6), limiting geometry

### Vertical Cutoff Rigidity

#### Method:

- Stoermer approximation
- $R = 14.3 \times \cos^4(\text{lat}_m)$ <sup>(4)</sup>

#### Weaknesses:

- Uses dipole approximation for Earth's geomagnetic field
- Assumes particle trajectory with normal incidence

#### Result:

- Improves charge resolution, but limits statistics in UH range

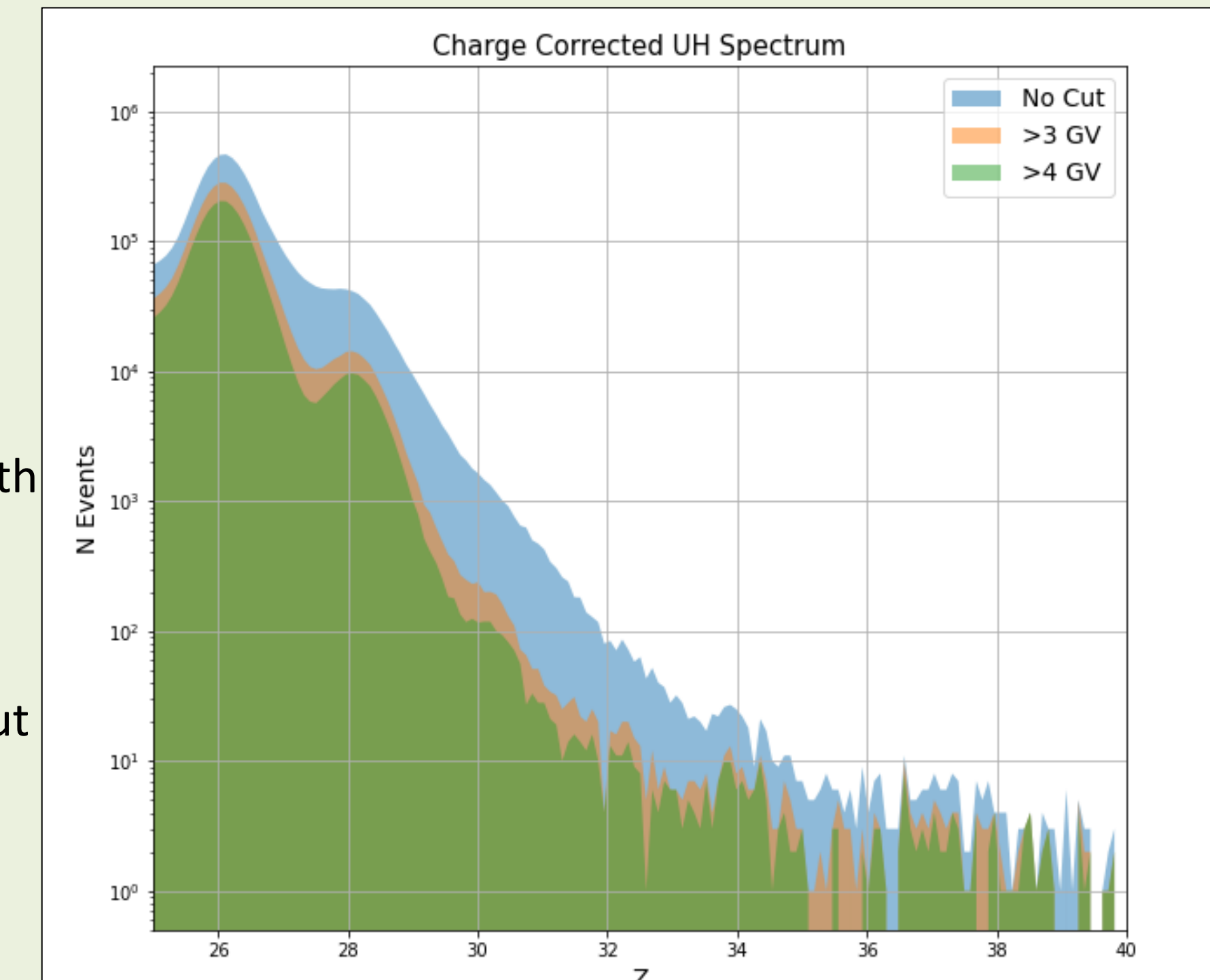


Figure 8: UH charge spectrum with no cut, a >3 GV cut, and a >4 GV cut.

## Calculating Effective Cutoff Rigidities

#### Method

- Numerically solve the equations of motion along a given trajectory for a range of rigidities to find allowed/forbidden trajectories<sup>(5)</sup>
  - Geomagnetic information calculated at each step using the IGRF13 and Tsyganenko 05 internal/external models

- Compute an effective cutoff rigidity<sup>(5)</sup> that considers the effect of the penumbra.
  - $R_E = R_L + (R_U - R_L) \times N_{\text{Forbidden}} / N_{\text{Total}}$

#### Result

- Updated rigidity cut improves charge resolution in the UH region, resulting in clearly resolved peaks for evenly charged nuclei up to Z=38
- Results are consistent with those using the TASC deposit method<sup>(6)</sup> despite the datasets having roughly 50 percent of events in common
- Future optimization and implementation of both methods will look to increase statistics while maintaining charge resolution

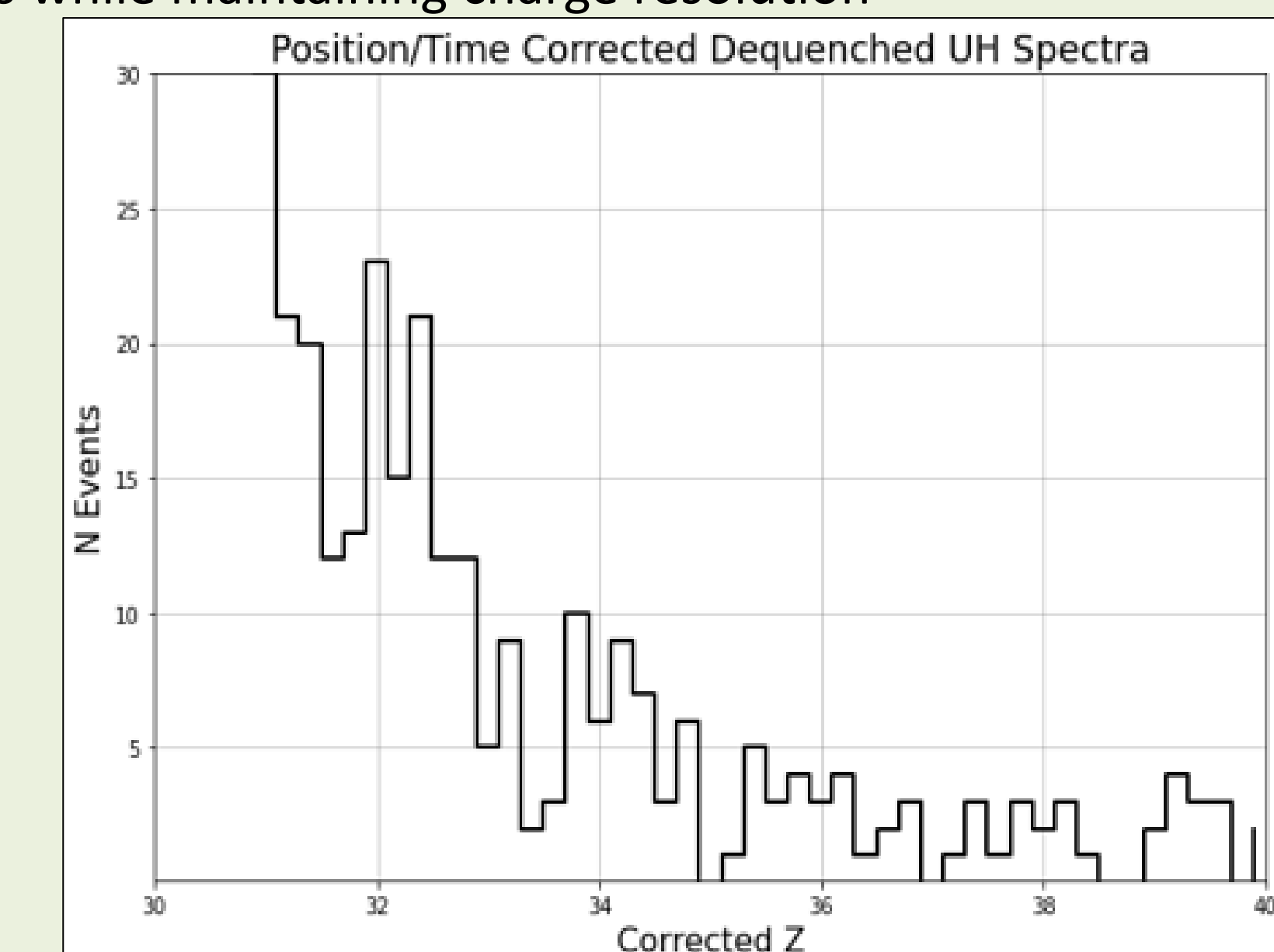


Figure 9: UH charge spectrum with a >4 GV rigidity cut using the calculated effect cutoff rigidities.

## References

- Y. Asaoka, S. Ozawa, and S. Torii et al. (CALET Collaboration), On-orbit operations and offline data processing of CALET onboard the ISS, *Astropart. Phys.* 100, 29-37 (2018).
- P. S. Marrocchesi et al. (CALET Collaboration), New results from the first 5 years of CALET observations on the International Space Station in *Proceedings of Science (ICRC2021; this conference)786*, (2021).
- B. F. Rauch and W. R. Binns et al. (CALET Collaboration), CALET Ultra Heavy Cosmic Ray Observations on the ISS, in *Proceedings of Science of The 36th International Cosmic Ray Conference* 130, (2019).
- D. J. Hoffmann and H. H. Sauer, Magnetospheric Cosmic-Ray Cutoffs and their Variations, in *Space Science Reviews*, 5-6:750-803, (1968)
- D. F. Smart, Changes in calculated vertical cutoff rigidities at the altitude of the international space station as a function of magnetic activity, in *Proceedings of Science ICRC 19907:337-340*, (1990)
- W. Zober, B. F. Rauch, A. Ficklin and N. Cannady et al. (CALET Collaboration), Progression Ultra-Heavy Cosmic-Ray Analysis with CALET on the International Space Station, in *Proceedings of Science (ICRC2021; this conference)1044*, (2021)

## Acknowledgements

We gratefully acknowledge JAXA's contributions to the development of CALET and to the operations onboard the ISS. We also wish to express our sincere gratitude to ASI and NASA for their support of the CALET project. This work is partially supported by JSPS Grant-in-Aid for Scientific Research (S) Number 26220708, JSPS Grant-in-Aid for Scientific Research (B) Number 17H02901, JSPS Grant-in-Aid for Scientific Research (C) Number 16K05382 and MEXT-Supported Program for the Strategic Research Foundation at Private Universities (2011-2015) S111021 in Waseda University. This work is also supported in part by MEXT Grant-in-Aid for Scientific Research on Innovative Areas Number 24103002. US CALET work is supported by NASA under RTOP 14-APRA14-0075 (GSFC) and grants NNX16AC02G (WUSL), NNX16AB99G (LSU), and NNX11AE06G (Denver).